Università degli Studi di Padova

Padua Research Archive - Institutional Repository

Oxidative stress by the mitochondrial monoamine oxidase B mediates calcium pyrophosphate crystal-induced arthritis

(Article begins on next page)

Venegas Francisca C (Orcid ID: 0000-0002-4198-3221)

Oxidative stress by the mitochondrial monoamine oxidase B mediates calcium pyrophosphate crystal-induced arthritis.

Running title: MAO-B mediates CPP-induced arthritis.

Francisca C. Venegas PhD[1,2#], Ricardo Sánchez-Rodríguez PhD [1,2#], Roberto Luisetto PhD [3], Roberta Angioni PhD [1,2], Antonella Viola PhD [1*], Marcella Canton PhD [1,2*]

[1]Department of Biomedical Sciences, University of Padua, 35131, Padua, Italy

[2]Fondazione Istituto di Ricerca Pediatrica Città della Speranza - IRP, 35129, Padua, Italy

[3]Department of Surgery, Oncology and Gastroenterology, University of Padua, 35131, Padua, Italy

[#] Francisca C. Venegas and Ricardo Sánchez-Rodríguez contributed equally to this work.

[*] Correspondence: marcella.canton@unipd.it and antonella.viola@unipd.it, Via Ugo Bassi, 58b, 35131 Padua PD, Italia.

ABSTRACT

Objective: Calcium pyrophosphate (CPP) crystal deposition in the joints is associated with a heterogeneous set of debilitating syndromes characterized by inflammation and pain, for which no effective therapies are currently available. As we found that the mitochondrial enzyme monoamine oxidase B (MAO-B) plays a fundamental role in promoting inflammatory pathways, this study aims at assessing the efficacy of two clinical-grade inhibitors (iMAO-Bs) in preclinical models of this disease, to pave the way for a novel treatment.

Methods: We tested our hypothesis in two murine models of CPP-induced arthritis, by measuring cytokine and chemokine levels, along with immune cell recruitment. iMAO-Bs (rasagiline and safinamide) were administered either before or after crystal injection. To elucidate the molecular mechanism, we challenged *in vitro* primed macrophages with CPP crystals and assessed the impact of iMAO-Bs in dampening proinflammatory cytokines and in preserving mitochondrial function.

Results: Both in preventive and therapeutic *in vivo* protocols, iMAO-Bs blunted the release of proinflammatory cytokines (interleukin (IL)-6 and IL1-β) and chemokines (CXCL10, CXCL1, CCL2 and CCL5) (n>6 mice/group). Importantly, they also significantly reduced ankle swelling (50.3% vs 17.1% [$P<0.001$] and 23.1% [$P=0.005$] for rasagiline and safinamide, respectively). Mechanistically, iMAO-Bs dampened the burst of reactive oxygen species (ROS) and the mitochondrial dysfunction triggered by CPP crystals in isolated macrophages. Moreover, iMAO-Bs blunted cytokine secretion and NLRP3 inflammasome activation through inhibition of the NF-κB and STAT3 pathways.

Conclusion: iMAO-Bs dampen inflammation in murine models of crystal-induced arthropathy, thereby uncovering MAO-B as a promising target to treat these diseases.

INTRODUCTION

Several acute and chronic arthropathies are associated with the deposition of calcium pyrophosphate dihydrate (CPP) crystals within joints and periarticular tissues (1). The most notable clinical manifestation of these arthropathies is acute CPP crystal arthritis (historically named *pseudogout*), which presents acute attacks of synovitis that clinically resemble a gout flare (2). CPP can also cause chronic inflammatory arthritis, with structural changes like those observed in osteoarthritis. Currently, only symptomatic treatments are available, and no effective therapies can prevent recurrent attacks or target the downstream pathogenic signals causing the clinical manifestations. Thus, there is an urgent and unmet need to develop novel treatments with minimal side effects and maximum efficacy.

CPP deposition is associated with excessive local production of extracellular inorganic pyrophosphate (PPi), often due to the increased activity of a regulator of extracellular PPi levels named ANKH (inorganic pyrophosphate transport regulator) (1). CPP crystals trigger the activation of the NLR family pyrin domain containing 3 (NLRP3, also named NALP3) inflammasome, resulting in the production of active interleukin (IL)-1β and IL-18 (3). Notably, an *in vivo* model of crystal-induced peritonitis in inflammasome-deficient mice showed an impaired neutrophil influx (3).

We recently found that hydrogen peroxide (H_2O_2) produced by the mitochondrial enzyme monoamine oxidase B (MAO-B) plays a nonredundant role in sustaining NLRP3 inflammasome activation (4). MAO catalyzes the oxidative deamination of neurotransmitters and dietary amines, generating aldehydes, ammonia and H_2O_2 (5). The two isoforms, MAO-A and MAO-B, differ in substrate specificity and inhibitor sensitivity. We have already shown that, in inflammatory conditions, the increased expression and activity of MAO overcomes cellular antioxidant defenses, altering redox homeostasis and eliciting deleterious effects (4). Mechanistically, MAO-B-driven production of H_2O_2 causes mitochondrial dysfunction and

Nuclear Factor kappa-light-chain-enhancer of activated B cells (NF-κB) activation, resulting in NLRP3 and pro-IL-1β overexpression (4). Using *in vitro* and *in vivo* approaches, we demonstrated that MAO-B inhibition by rasagiline prevents IL-1β secretion in response to lipopolysaccharide (LPS), and that MAO-B-deficient mice have an impaired response to LPS-mediated endotoxemia (4).

Here, we investigated whether targeting MAO-B could dampen inflammation in different experimental models of CPP-induced arthropathies. To this aim we used both rasagiline and safinamide, which are irreversible and reversible inhibitors, respectively.

MATERIAL AND METHODS

Reagents and antibodies

Ultrapure LPS from *Escherichia coli* (Sigma Aldrich), ATP (Sigma Aldrich), rasagiline (Abcam), Trolox (6-hydroxy-2,5,7,8-tetramethylchroman-2-carboxylic acid) (Sigma Aldrich), CM-H$_2$DCF-DA (5-(and-6)-chloromethyl-2',7'-dichlorodihydrofluorescein diacetate, acetyl ester), TMRM (tetramethylrhodamine, methyl ester) (Thermo Fisher Scientific), CPP crystals (Invivogen). Safinamide was kindly provided by Zambon SpA, Italy. The following antibodies were used: polyclonal rabbit anti-phosphoNF-κB (3033, Ser536, Cell Signaling), monoclonal anti-H4 and polyclonal rabbit anti-STAT3 (Abcam), goat anti-rabbit IgG-HRP (GE Healthcare). Monosodium Urate (MSU) crystals were kindly provided by Dr. Anna Scanu and were obtained as described in (6).

Mice and *in vivo* treatments

Wild-type C57BL/6 (males, 8-10 weeks old) were obtained from Jackson Laboratories, and were maintained in the animal facility of the *Istituto di Ricerca Pediatrica, Fondazione Città della Speranza,* at controlled temperature, with a 12-on/12-off light cycle with access to water and food *ad libitum*. All experiments followed committee guidelines and the institutional

protocols for animal care, that was approved by Ministero della Salute (538/2020-PR). Mice were randomly allocated to treatment groups after age and sex matching.

Air-pouch mouse model

The air pouch was formed as previously described (7). Briefly, 3.5 ml of sterile air were injected subcutaneously into the murine back, and after three days the procedure was repeated. At day 7, mice were randomly separated into 4 groups and were treated with: i) 1 ml sterile phosphate buffer saline solution (PBS), injected inside the dorsal air pouch (n=6), ii) a CPP crystal suspension (2 mg in 1 ml PBS, injected inside the dorsal air pouch, (n=8), iii) rasagiline (2.5 mg/kg; *per os*) followed by CPP crystal injection as in ii) (CPP + ras, n=6) or iv) safinamide (40 mg/kg; *per os*) followed by CPP crystal injection as in ii) (CPP + saf, n=7). All the injections were performed in anesthetized mice [Sevorane®] using a Fluovac respiratory system and microliter syringes with 27 G beveled needles. Three hours later, the animals were euthanized in a CO_2 chamber, and air pouches were washed with 1 ml PBS. The exudate was collected for myeloid cell subset characterization and for cytokines and chemokines quantification. Furthermore, a biopsy was collected from the retroperitoneal membrane to measure the gene expression of cytokines and chemokines.

CPP crystal-induced arthritis mouse model

Mice were injected with a suspension of sterile CPP crystals (0.3 mg in 20 µl PBS) into the right ankle joint. Injections were performed under inhalant anesthesia (Sevorane®) using a Fluovac respiratory system and microliter syringes with 27G beveled needles. Mice were randomized into 4 groups receiving: CPP crystals (intra-articular, i.a; CPP group; n=10), CPP crystals + rasagiline (1.25 mg/kg; *per os*, n=10), CPP crystals + safinamide (20 mg/kg; *per os*, n=9) and PBS (i.a; control group, n=3). iMAO-Bs were administered at various time points after injection (1-6-24-30 h). Ankle swelling was measured at 0-6-24-30 h using a precision digital caliper (Kroeplin Gmbh). To avoid any bias, ankle swelling was measured blindly.

Forty-eight hours after crystal injection mice were euthanized, and ankle joint tissue was collected for cytokine and chemokine gene expression analysis.

Cell preparation and stimulation

Immortalized macrophages (iμϕ) were obtained and cultured as described (8). Briefly, cells ($2x10^6$) were pretreated with or without rasagiline (20 μM), safinamide (10 μM) or Trolox (0.5 mM) for 15 min. Then iμϕ were primed with LPS (200 ng/ml) for 2.5 h and subsequently added with CPP crystals (LPS/CPP) (250 μg/ml).

Reactive Oxygen Species (ROS) detection

iμϕ cells ($1x10^6$) were seeded and incubated with rasagiline (20 μM), safinamide (10 μM) or Trolox (0.5 mM) for 15 min in RPMI 2% FCS, followed by LPS priming and CPP crystal challenge as described above. After 2 h, iμϕ were loaded with CM-H$_2$DCF-DA (2.5 μM) for 30 min to detect ROS levels. Upon washing, iμϕ images were acquired with a Leica DMI6000B microscope (Wetzlar, Germany), equipped with a digital camera. 540±20 nm excitation and 590 nm long-pass emission filter settings were used. The mean fluorescence intensity of single cells (15-40 randomly chosen for each condition) was quantified in 4-6 fields per coverslip. Data were analyzed using Metafluor software (Universal Imaging).

Mitochondrial membrane potential assessment

Mitochondrial membrane potential (ΔΨm) assessment is based on TMRM accumulation, as described (9). iμϕ cells ($1x10^6$) were incubated with rasagiline (20 μM), safinamide (10 μM) of Trolox (0.5 mM) for 15 min in RPMI 2% FCS, followed by LPS/CPP as indicated in the legend. To measure ΔΨm, they were incubated with serum-free media supplemented with 50 nM TMRM for 30 min, and fluorescence images were acquired with a Leica DMI6000B microscope. Data were analyzed using Metafluor software (Universal Imaging). 560±20 nm excitation and 645±37 nm emission filter settings were used. Clusters of mitochondria were identified as regions of interest (ROI). To exclude artifacts due to different loading capacity of

the cells, sequential images were acquired before and after carbonyl cyanide-p-trifluoromethoxy-phenylhydrazone (FCCP, 4 μM) addition. ΔΨm was estimated as the difference in TMRM fluorescence intensity of ROI before and after FCCP.

Flow cytometry analysis

Cells collected from peritoneal exudates were washed in PBS and centrifuged (5 min at 400 g). Red blood cells were lysed with ACK lysing solution (Lonza), Fc-receptor was blocked (anti-mouse CD16/32, BD) before the staining protocol. Flow cytometric analysis was performed with the following antibodies incubated for 20 min at 4°C: anti-CD11b-PE-cy7 (clone M1/70), anti-LY6G-APC-96 Cy7 (clone 1A8), anti-F4/80-FITC (clone CI: A3-1) into BD Truecount™ tubes according to manufacturer instructions. Samples were acquired with FACSCanto and analyzed with FlowJo software (Tree Star, Inc.). Absolute numbers of infiltrating cells were calculated according to BD Truecount™ specifications. Briefly, absolute count of the cell population was obtained by dividing the number of positive cell events by the number of bead events, and then multiplying by the BD Trucount™ bead concentration (number of beads/test volume). Data are expressed as % of number of cells from CPP or CPP+rasagiline or safinamide on number of cells from PBS-treated mice.

ASK speck formation

ASC-mCherry macrophages were a kind gift from P. Pelegrin (Instituto Murciano de Investigación Biosanitaria, Spain). Briefly, cells ($5x10^4$) were treated with LPS (200 ng/ml) for 2.5 h and CPP (250 μg/ml) or MSU (500 μg/ml) for 6 h. Then, cells were fixed with cold acetone for 5 min and nuclei were stained with Hoechst 33342. Images were acquired with a Zeiss LSM800 confocal microscope. ASC specks were detected and quantified with ZEN 3.0 software and normalized over total ASC-mCherry positive macrophages *per* field.

Quantitative real-time PCR

RNA was isolated with TRIzol (Invitrogen) according to the manufacturer's instructions. cDNA was obtained with random primers and High-Capacity cDNA Reverse Transcription Kit (Thermo Fisher), quantitative PCR was performed with specific primers by SYBR Green PCR Master Mix (Applied Biosystems) in ABI PRISM 7500 real-time PCR system (Applied Biosystems). *Il6* reverse 5'-GCCATTGCACAACTCTTTTCTC forward 5'-AGGATACCACTCCCAACAGAC; *Il1β* reverse 5'-TTGTTCATCTCGGAGCCTGTAG forward 5'-GGACATGAGCACCTTCTTTTCC; *Irg1* reverse 5'-ACAGTGCTGGAGGTGTTGGAAC forward 5'-GGTATCATTCGGAGGAGCAAGAG (10); *Cxcl 10* reverse 5'-GACCTTTTTTGGCTAAACGCTTTC forward 5'-ATCATCCCTGCGAGCCTATCCT; *Cxcl1* reverse 5'-AACCAAGGGAGCTTCAGGGTCA forward 5'-TCCAGAGCTTGAAGGTGTTGCC (11); *Trem1* reverse 5'-CGGGTTGTAGTTGTGTCACTGG forward 5'- CCTGTTGTGCTCTTCCATCCTG; *Tnf* reverse 5'-CGGATCATGCTTTCTGTGCTC forward 5'-GAAAAGCAAGCAGCCAACCA; *Puma* reverse 5'-CTGTTTCCACCTCAAGTCCTGG forward 5'-CATAGTTGTCCGTCAGGAACGG ; *Ccl2* reverse 5'-GCATTAGCTTCAGATTTACGG forward 5'-TTAAAAACCTGGATCGGAACC and *Gapdh* reverse 5'-CCTTGACTGTGCCGTTGAATTT forward 5'-GCAAAGTGGAGATTGTTGCCAT. Data were normalized on the *Gapdh* gene expression using the comparative ΔΔCt method.

Immunoblot analysis

Nuclear extracts from each cell line (4x10^6) were prepared as previously described (12). Protein nuclear extracts (5 μg) were separated by 4–12% Bold NuPage (Thermo Fisher Scientific) polyacrylamide gels and transferred onto polyvinylidene difluoride (PVDF) 0.22 μm membranes (Bio-Rad). Then, membranes were processed with a blocking solution with 3% bovine serum albumin (Sigma Aldrich) in tris buffer saline (TBS) and incubated overnight with primary antibodies (1:1000) at 4°C. Then, membranes were incubated with anti-rabbit

peroxidase-conjugated secondary antibodies (GE Healthcare). Chemiluminescence was obtained by the intensive chemiluminescence kit (GE Healthcare), and images were obtained with ImageQuant LAS 500 (GE Healthcare).

Luminex assay

25 analytes (G-CSF, GM-CSF, IFN-γ, IL-1α, IL-1β, IL-2, IL-4, IL-5, IL-6, IL-7, IL-9, IL-10, IL-12 (p40), IL-12 (p70), IL-13, IL-15, IL-17, IP-10, CXCL5, MCP-1, MIP-1α, MIP-1β, MIP-2, RANTES, TNF-α) were analyzed by Luminex assay (Millipore, Billerica, USA) in the air pouch exudates. The diluted standards and quality controls were used according to the manufacturer's instructions. The plate was read on Luminex 200™. Analysis was performed using xPONENT 3.1 software.

Statistics

Data are presented as mean ± standard error of the mean (SEM). All analyses were performed with a statistical software package (GraphPad Prism), using one-way ANOVA with Tukey's post-hoc test or Kruskal-Wallis with Dunn's post-hoc test or two-tailed unpaired t test. $*P<0.05$, $**P<0.01$, $***P<0.005$, $****P<0.001$. For heatmap hierarchical clustering was calculated by "Manhattan" distances.

RESULTS

The anti-inflammatory efficacy of two MAO-B inhibitors (iMAO-Bs), rasagiline and safinamide, was initially tested in the air-pouch experimental model of acute crystal-induced inflammation (7). Mice were randomized in groups receiving rasagiline, safinamide or vehicle *per os* and then injected with CPP crystals into the air-pouches. The cytokine and chemokine levels in the air pouch exudate were quantitated 3 hours later, along with the inflammatory cells (Fig. 1a). We found that pretreatment with iMAO-Bs hinders the production of several proinflammatory cytokines, chemokines, and growth factors in response to crystal stimulation

(Fig. 1b, suppl 1, suppl 2). Moreover, MAO-B inhibition prevents the recruitment of monocytes, macrophages, and granulocytes into the air pouch (Fig. 1c-h, suppl 3).

These preliminary results suggest that MAO-B is a potential therapeutic target in human arthropathies. To test the therapeutic efficacy of iMAO-Bs, we exploited a more complex experimental animal model, in which mice were injected with CPP crystals into the ankle joint, then treated or not with iMAO-Bs, and finally sacrificed 48 hours later (Fig. 1i). Both rasagiline- and safinamide-treated mice showed a significant decrease in ankle swelling at 48 hours (Fig. 1j). Notably, iMAO-Bs dampened the expression levels of cytokines and chemokines involved in ankle tissue inflammation (Fig. 1k).

To gain more insight into the molecular mechanism responsible for the anti-inflammatory efficacy of iMAO-Bs, we challenged primed immortalized macrophages with CPP crystals. CPP crystals triggered a rapid increase in ROS levels in macrophages, which was followed by a collapse of the mitochondrial membrane potential (Fig. 2a-b). Notably, iMAO-Bs prevented both the increase in ROS levels and the mitochondrial depolarization elicited by crystals, highlighting a crucial role of MAO-B in controlling mitochondrial performance. The antioxidant Trolox showed similar efficacy, suggesting a ROS-driven mechanism (Fig. 2a). Since ROS can trigger NF-κB, which is a master transcription factor inducing the expression of proinflammatory genes, and having already shown that MAO-B activity is necessary to trigger NF-kB in response to LPS (4), we wondered whether MAO-B could affect the activation of the NF-κB pathway induced by CPP stimulation. Indeed, we found that iMAO-Bs dampened crystal-induced NF-κB activation (Fig. 1c). Interestingly, iMAO-Bs also inhibited STAT-3 activation, a transcription factor involved in IL-6 activation (Fig. 1c). In accordance with these results as well as with the *in vivo* data, we found that rasagiline and safinamide decreased crystal-induced release of IL-1β and IL-6 (Fig. 2d-e), and inhibited ASC-speck formation, which is a classical readout for NLRP3 inflammasome activation (Fig. 2f). Similar results were

obtained using MSU crystals (suppl 4). Altogether, these data indicate that, in response to CPP crystals, MAO-B activity is required for the generation of ROS that initiate the inflammatory response by activating key transcription factors (NF-κB and STAT-3) and the NLRP3 inflammasome.

DISCUSSION

Our findings show that iMAO-Bs strongly dampen the inflammatory phenotype of two complementary different experimental murine models of crystal-induced arthritis. The subcutaneous air-pouch model resembles a joint capsule and mimics the acute inflammation related to bursitis, where neutrophils predominate. The inflammation onset is extremely rapid and self-limiting within a few hours (7). The second model that we exploited, the experimental arthritis induced by microcrystals, is more complex, involving synoviocytes, cartilage and bone. The inflammatory stimulus induces an increase in the vascular permeability, which supports the inflammation and reaches its peak 48 hours after the stimulus. The marked inhibition of CXCL10 is particularly interesting in our preclinical models, as this chemokine plays a crucial role in arthritis, being involved in joint inflammation and bone destruction (13). Mechanistically, we provided evidence that ROS produced by MAO-B mediate the activation of NF-κB and STAT-3, two transcription factors crucial for the amplification of the pro-inflammatory response. Recent studies strengthen the significance in human diseases of the synergistic activation of NF-κB and STAT3 and identify this pathway as a fundamental mechanism to enhance inflammation in several diseases, including cytokine storm syndromes, autoimmune diseases, and cancer (14).

Taken together, our results indicate that the inhibition of the mitochondrial enzyme MAO-B may represent a valid therapeutic strategy for the treatment of arthropathies associated with the deposition of CPP crystals, as these drugs act both through a preventive and a therapeutic

protocol. Targeting MAO-B offers several advantages over other compounds: a) it prevents the formation of a specific subset of mitochondrial ROS that becomes excessive in pathological conditions, in contrast to general antioxidants that scavenge ROS in a nonspecific manner, thereby affecting also important ROS-driven functions; b) it hampers mitochondrial dysfunction triggered by CPP crystals, thus limiting the accumulation of damaged mitochondria, and, potentially, mitochondrial DAMP release; c) rasagiline and safinamide are well tolerated and are used in clinics to treat Parkinson's disease (15). Finally, preclinical studies showed that MAO-B deficient mice are protected against cardiac dysfunction (16). These findings suggest another possible advantage, as acute CPP crystal arthritis is significantly associated with an elevated risk for cardiovascular events (17).

The main limitation of this study is that the efficacy of iMAO-Bs has been assessed in experimental models of the disease. Further studies will be aimed at validating the role of MAO-B in cells from patients affected by these crystal-arthropathies.

In summary, we believe that repurposing iMAO-Bs would allow a fast and safe approach to treat crystal-arthritis and other inflammatory diseases characterized by IL-1β-driven pathology.

ACKNOWLEDGEMENTS

REFERENCES

1.   McCarthy G.M. and Dunne A., *Calcium Crystal Deposition Diseases - Beyond Gout.* Nat Rev Rheumatol, 2018. **14**(10): p. 592-602.

2.   Oliviero F., Bindoli S., Scanu A., et al., *Autoinflammatory Mechanisms in Crystal-Induced Arthritis.* Front Med (Lausanne), 2020. **7**: p. 166.

3.   Martinon F., Petrilli V., Mayor A., et al., *Gout-Associated Uric Acid Crystals Activate the Nalp3 Inflammasome.* Nature, 2006. **440**: p. 237-41.

4.   Sanchez-Rodriguez R., Munari F., Angioni R., et al., *Targeting Monoamine Oxidase to Dampen Nlrp3 Inflammasome Activation in Inflammation.* Cell Mol Immunol, 2021. **18**: p. 1311-13.

5.   Youdim M.B., Edmondson D., and Tipton K.F., *The Therapeutic Potential of Monoamine Oxidase Inhibitors.* Nat Rev Neurosci, 2006. **7**: p. 295-309.

6.   Scanu A., Oliviero F., Gruaz L., et al., *High-Density Lipoproteins Downregulate Ccl2 Production in Human Fibroblast-Like Synoviocytes Stimulated by Urate Crystals.* Arthritis Res Ther, 2010. **12**: p. 1-10.

7.   Hall C.J., Sanderson L.E., Lawrence L.M., et al., *Blocking Fatty Acid-Fueled Mros Production within Macrophages Alleviates Acute Gouty Inflammation.* J Clin Invest, 2018. **128**: p. 1752-71.

8.   Spera I., Sanchez-Rodriguez R., Favia M., et al., *The J2-Immortalized Murine Macrophage Cell Line Displays Phenotypical and Metabolic Features of Primary Bmdms in Their M1 and M2 Polarization State.* Cancers, 2021. **13**: p. 5478.

9.   Sorato E., Menazza S., Zulian A., et al., *Monoamine Oxidase Inhibition Prevents Mitochondrial Dysfunction and Apoptosis in Myoblasts from Patients with Collagen VI Myopathies.* Free Radic Biol Med, 2014. **75**: p. 40-7.

10.   Pessler F., Mayer C.T., Jung S.M., et al., *Identification of Novel Monosodium Urate Crystal Regulated Mrnas by Transcript Profiling of Dissected Murine Air Pouch Membranes.* Arthritis Res Ther, 2008. **10**(3): p. R64.

11.   Cohen K., Mouhadeb O., Shlomo S.B., et al., *Commd10 Is Critical for Kupffer Cell Survival and Controls Ly6chi Monocyte Differentiation and Inflammation in the Injured Liver.* Cell Rep, 2021. **37**: p. 110026.

12.   Sanchez-Rodriguez R., Tezze C., Agnellini A.H.R., et al., *Opa1 Drives Macrophage Metabolism and Functional Commitment Via P65 Signaling.* Cell Death Differ, 2022; **30**, p. 742–52.

13.   Lee J.H., Kim B., Jin W.J., et al., *Pathogenic Roles of Cxcl10 Signaling through Cxcr3 and Tlr4 in Macrophages and T Cells: Relevance for Arthritis.* Arthritis Res Ther, 2017. **19**(1): p. 163.

14.   Murakami M., Harada M., Kamimura D., et al., *Disease-Association Analysis of an Inflammation-Related Feedback Loop.* Cell Rep, 2013. **3**(3): p. 946-59.

15.   Finberg J.P.M., *Inhibitors of Mao-B and Comt: Their Effects on Brain Dopamine Levels and Uses in Parkinson's Disease.* J Neural Transm, 2019. **126**(4): p. 433-48.

16.   Kaludercic N., Carpi A., Nagayama T., et al., *Monoamine Oxidase B Prompts Mitochondrial and Cardiac Dysfunction in Pressure Overloaded Hearts.* Antioxid Redox Signal, 2014. **20**(2): p. 267-80.

17.   Tedeschi S.K., Huang W., Yoshida K., et al., *Risk of Cardiovascular Events in Patients Having Had Acute Calcium Pyrophosphate Crystal Arthritis.* Ann Rheum Dis, 2022. **81**(9): p. 1323-9.

Figure legends

Fig. 1. (a) Schematic overview of murine air-pouch model of acute CPP-induced inflammation. Mice were air-injected to form the pouch. After 6 days, they were treated with rasagiline (ras), safinamide (saf) or vehicle and 15 min later injected with CPP crystals). CPP-untreated mice served as control (unst). Mice were sacrificed after 3 hours.

(b) Proinflammatory chemokines and cytokines release measured by Luminex Multiplex assay in pouch exudate. Heat map (*left*) represents unsupervised clustering cytokine/chemokine concentration Specific bar graphs (*right*) from the heat-map data (n=4 independent experiments).

(c-h) Flow cytometry analysis of the myeloid subsets in the pouch exudates (n=3 independent experiments).

(i) Outline of CPP-induced arthritis murine model. Mice were injected with CPP crystals in the ankle (0 h) and treated with rasagiline, safinamide or vehicle, at various time points (1-6-24-30 h). CPP-untreated mice served as control. Mice were sacrificed 48 h post-crystal injection.

(j) Ankle swelling measurement of mice treated as in (i)

(k) Proinflammatory cytokine and chemokine relative gene expression in ankle tissues from mice treated as in (i) (48 h after CPP injection). *Gapdh* was used as housekeeping. Data are presented as mean±SEM. Statistical analysis was performed with one-way ANOVA with Tukey's post hoc test *P < 0.05, **P < 0.01, ***P < 0.005, ****P < 0.001.

Fig. 2 (a) Immortalized macrophages (iμφ) primed with LPS and CPP crystals (LPS/CPP) in the presence or absence of rasagiline, safinamide or Trolox. ROS levels were detected in iμφ stained with DCF-DA. Values are presented as the fold-changes of unstimulated cells (unst) (n=3 independent experiments).

(b) Mitochondrial membrane potential ($\Delta\Psi$) was measured with TMRM in iμϕ treated as in (a), images were acquired before and after FCCP addition. The graph reports the difference in fluorescence intensities before and after FCCP. Values are reported as relative intensity to unstimulated cells (n=3 independent experiments).

(c) Representative Western blot for STAT-3 and NF-κB (P65) in nuclear protein extracts from iμϕ treated as in (a). Histone 4 (H4) was used as a loading control. (d-e) IL-1β and IL-6 release levels in supernatants from iμϕ treated as in (a) (n=3 independent experiments).

(f) Representative images (*right*) and quantification of ASC specks (*left*) in ASC-mCherry macrophages (n=3 independent experiments), treated as in (a). Data are presented as mean±SEM. Statistical analysis was performed with one-way ANOVA with Tukey's post hoc test (d-f) and the Kruskal–Wallis test with Dunn's post hoc test (a-b) *P < 0.05, **P < 0.01, ***P < 0.005, ****P < 0.001.
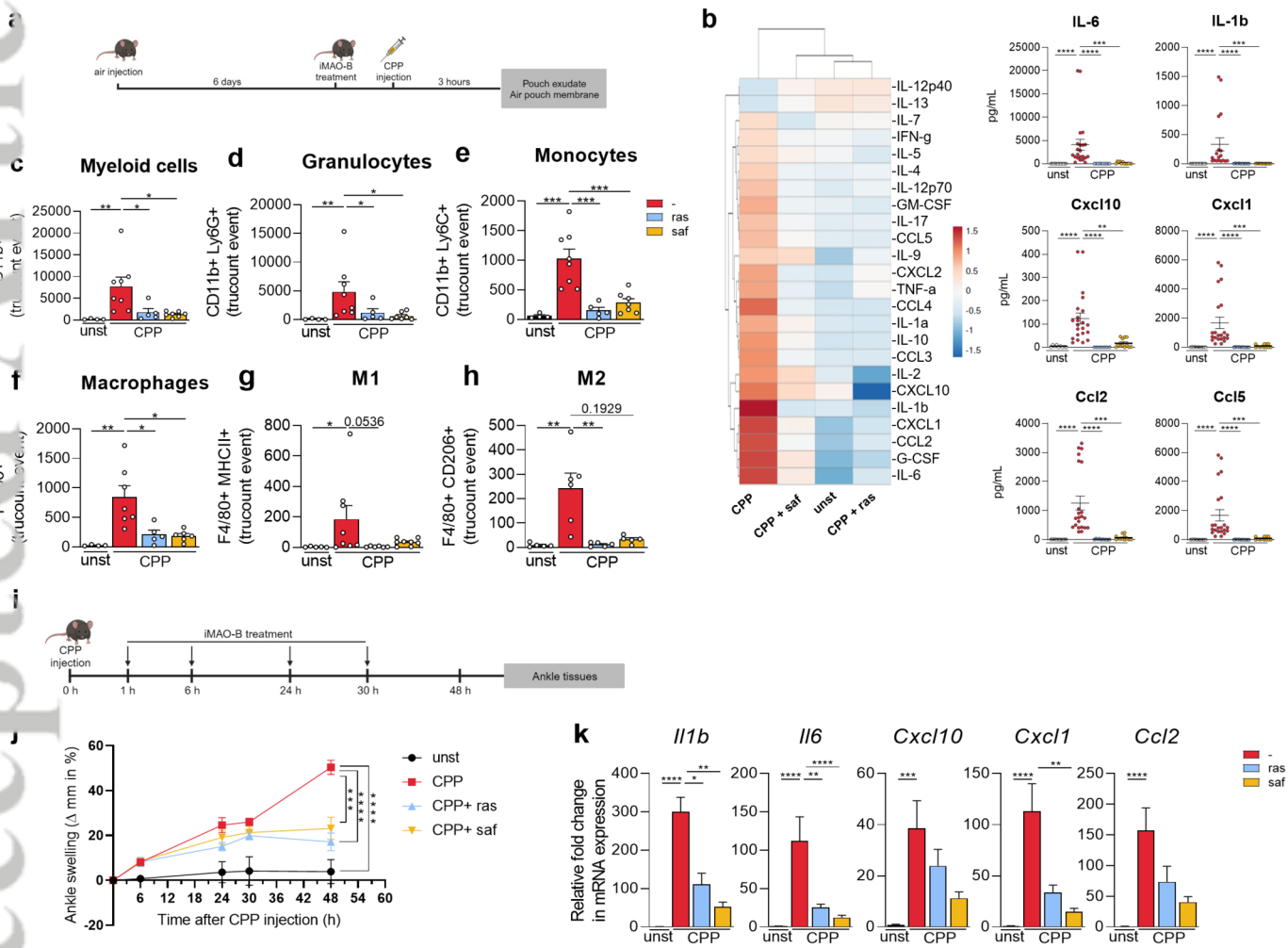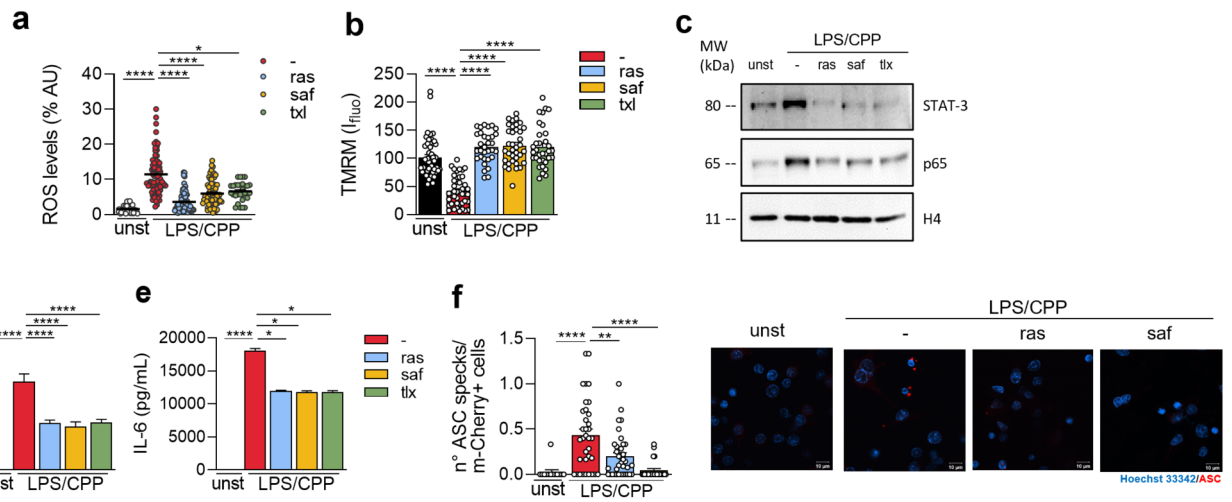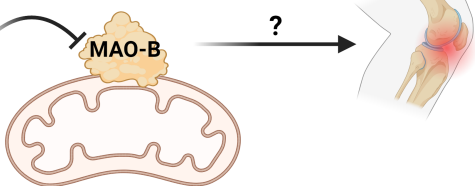
Figure1 (2).tif

Figure2 (2).tif

Oxidative Stress by the Mitochondrial Monoamine Oxidase B Mediates Calcium Pyrophosphate Crystal-Induced Arthritis
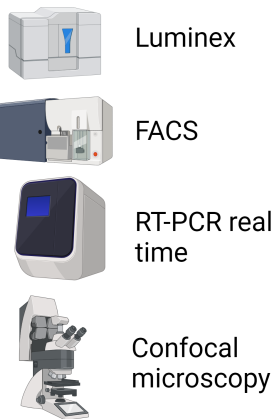
Objective

-Rasagiline
-Safinamide

MAO-B

?

Asses the efficacy of two clinical-grade inhibitors (iMAO-Bs) in preclinical models of calcium pyrophosphate dihydrate (CPP) crystals deposition disease.
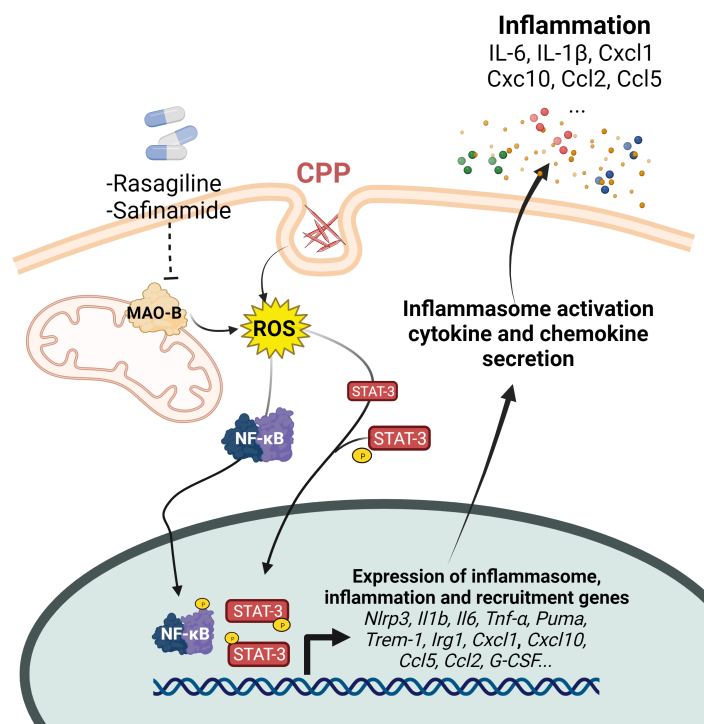
Methods

CPP Crystals

Air-pouch model → Luminex

Induced arthritis model → FACS

→ RT-PCR real time

-iμφ → Confocal microscopy

Results

Inflammation
IL-6, IL-1β, Cxcl1
Cxc10, Ccl2, Ccl5
...

-Rasagiline
-Safinamide

CPP

MAO-B

ROS

Inflammasome activation cytokine and chemokine secretion

STAT-3

NF-κB

STAT-3

Expression of inflammasome, inflammation and recruitment genes
Nlrp3, Il1b, Il6, Tnf-α, Puma, Trem-1, Irg1, Cxcl1, Cxcl10, Ccl5, Ccl2, G-CSF...

NF-κB

STAT-3

STAT-3

Venegas C, Sánchez-Rodríguez R, Luisetto R, et al. Oxidative stress by the mitochondrial monoamine oxidase B mediates calcium pyrophosphate crystal-induced arthritis. Arthritis Rheumatol 2023.

Arthritis & Rheumatology

AMERICAN COLLEGE of RHEUMATOLOGY
Empowering Rheumatology Professionals

Venegas graphical abstract 23-0672.png